Journal of Fluorine Chemistry xxx (2015) xxx–xxx

Contents lists available at ScienceDirect

Journal of Fluorine Chemistry

journal homepage: www.elsevier.com/locate/fluor

Delineating the physical organic profile of the 6-fluoro glycosyl donor

Nico Santschi [a,b], Nuria Aiguabella [a,b], Vanessa Lewe [a], Ryan Gilmour [a,b,*]

[a] Institute for Organic Chemistry, Westfälische Wilhelms-Universität Münster, Correnstrasse 40, 48149 Münster, Germany
[b] Excellence Cluster EXC 1003 "Cells in Motion", Westfälische Wilhelms-Universität Münster, Correnstrasse 40, 48149 Münster, Germany

ARTICLE INFO

Article history:
Received 16 April 2015
Received in revised form 26 May 2015
Accepted 3 June 2015
Available online xxx

Dedicated to Professor Véronique Gouverneur on her receipt of the 2015 ACS Award for Creative Work in Fluorine Chemistry.

Keywords:
Carbohydrates
Fluorine
Glycosylation
Physical organic chemistry
Stereoelectronic effects

1. Introduction

Fluorinated glycostructures are emerging as valuable mimics of natural carbohydrates on account of their enhanced lipophilicity and the minimal steric disruption that results from hydroxyl to fluorine substitution [1–3]. The ability to subtly modulate the hydrogen bond network of the glycostructure without altering the overall topology of the scaffold renders fluorine incorporation attractive as a molecular editing strategy [4]. Effective synthetic methods to construct complex fluorinated carbohydrates are required to meet the demands of this expanding research field. Unlike their natural counterparts, very little is known about the behavior of fluorinated glycosyl donors, and the effect this seemingly innocuous [OH → F] switch has on a glycosylation process. To reconcile this dearth of information with the growing interest in fluorinated carbohydrates [5], the 6-deoxy-6-fluoroglycosyl donor **1** was selected as a model compound for a physical organic analysis, and compared to the common 6-benzyloxy derivative that is routinely used in preparative glycochemistry. 6-Deoxy-6-fluoroglucose building blocks have found widespread application in a variety of disciplines ranging from mechanistic enzymology [6], and glycopeptide antigen design [7] through to radiotracers for nuclear medicine [8]. Moreover, from the perspectives of conformation and reactivity, they are intriguing candidates for investigation on account of the vicinal relationship that links the fluorine atom to an electropositive centre (F–C_β–C_α–O–) via a freely rotatable (exocyclic) bond. Fluorinated scaffolds bearing an electron withdrawing substituent in the β-position are known to adopt conformations that benefit from stabilising hyperconjugative ($\sigma_{C-H} \rightarrow \sigma_{C-F}^*$) and electrostatic interactions ($F^{\delta-}\cdots O^{\delta+}$): this is commonly referred to as the *gauche* effect [9]. These effects may conceivably be exploited to control glycosylation selectivity: this notion has been validated in the corresponding 2-deoxy-2-fluoro systems [10]. To explore the role of the 6-fluoro substituent in a conventional glycosylation reaction, the trichloroacetimidate donor **1** was selected as a platform for investigation (Fig. 1). Stereoelectronic considerations suggest that the conformational equilibrium in **1** would likely favor conformers **I** and **II** over **III**. Indeed, of the three staggered conformers partitioned by 120°, the *syn-clinal endo* arrangement **I** would likely predominate on account of the stabilizing $\sigma_{C-H} \rightarrow \sigma_{C-F}^*$ hyperconjugative interaction. Assuming a mechanism with

* Corresponding author at: Westfälische Wilhelms-Universität Münster, Institute for Organic Chemistry Correnstrasse 40, 48149 Münster, Germany. Tel.: +49 251 83 33271.
E-mail address: ryan.gilmour@uni-muenster.de (R. Gilmour).

http://dx.doi.org/10.1016/j.jfluchem.2015.06.004

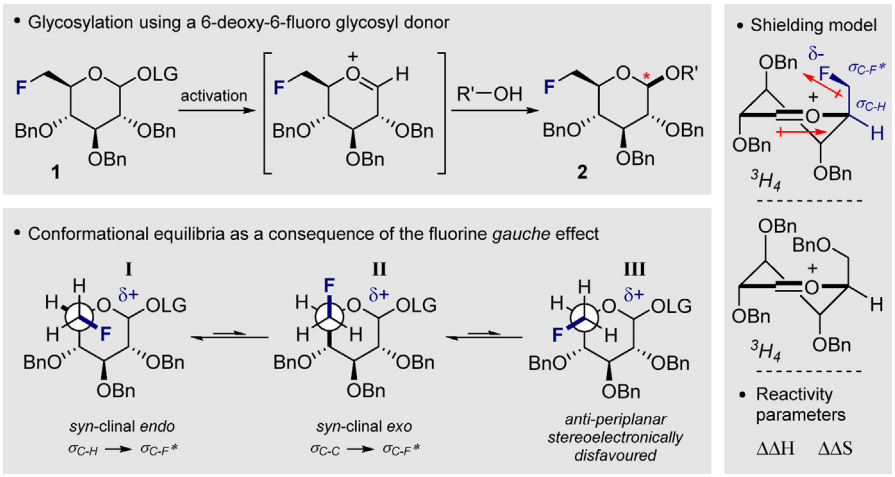

Fig. 1. The fluorine *gauche* effect in the 6-deoxy-6-fluoro glycosyl donor **1**. LG = leaving group (trichloroacetimidate).

significant S_N1 character [10c], the incipient oxocarbenium ion would likely benefit from dipole minimization thus placing the highly electronegative fluorine substituent proximal to the electrophilic (sp^2) anomeric centre. Extensive studies by the Woods and Woerpel groups have demonstrated that the $^3H_4$ conformation of the *per*-benzylated glucose-derived oxocarbenium ion benefits from electrostatic stabilization arising from the axial benzyloxy groups [12]; this would enforce an axial arrangement of the mono-fluoromethyl substituent thus augmenting the [C–F → C=O$^+$] dipole minimization and increasing proximity to the anomeric carbon (Fig. 1, right). In the case of the 6-OBn analog, conformer **I** should also predominate on account of the $\sigma_{C-H} \rightarrow \sigma_{C-OBn}{}^*$ hyperconjugative interaction. However this conformational preference may be less pronounced on account of the the poorer acceptor capabilities of the $\sigma_{C-OBn}{}^*$ orbital, and the larger steric demands of the benzyloxy group (cf. fluorine). These considerations may lead to the $^3H_4$ transition state being favored over the $^4H_3$ when substituting benzyloxy by fluorine: this ought to be reflected in enhanced β-selectivity. Since the fluorine substituent is generally perceived as having a small steric footprint, a top-face attack on the $^3H_4$ oxocarbenium ion intermediate according to the Fürst–Plattner rule should be less hindered than in the corresponding OBn-substituted system (see Scheme 3).

Herein, we report a variable temperature glycosylation selectivity study for the 6-deoxy-6-fluoroglucose donor **1** in a model reaction and validate the fluorine substituent as a useful steering group in chemical glycosylation. By extrapolation of the associated entropic ($\Delta\Delta S_{\beta\alpha}{}^{\ddagger}$) and enthalpic ($\Delta\Delta H_{\beta\alpha}{}^{\ddagger}$) parameters, a comparison can be made with the corresponding 6-benzyloxy system that is commonly employed in preparative glycochemistry.

2. Results and discussion

The synthesis of fluorinated donor **9** began with the *per*-benzylation of commercially available methyl 4,6-*O*-benzylidene-α-D-glucopyranoside (**3**). Under standard reaction conditions with NaH, BnBr and TBAI in DMF, the desired product **4** was isolated in 85% yield after low-temperature recrystallization from ether/pentane [13]. Subsequently, regioselective reduction of the benzylidene acetal afforded the free 6-hydroxyl derivative in 90% yield relying on a combination of catalytic amounts of $Cu(OTf)_2$ and 5 equivalents of BH_3·THF in CH_2Cl_2 at 0 °C [14]. The fluorination of compound **5** had previously been described with DAST at 70 °C [15]. However, due to the thermal instability of this reagent at elevated temperatures [16], an alternative protocol was explored relying on the addition of Deoxofluor™ at 0 °C, followed by stirring at 70 °C [17]. This proved successful in delivering the fluorinated product **6** in 76% yield as a white solid. Attempts to hydrolyse the methyl acetal of **6** to the corresponding lactol (C1–OH) **8** proved difficult [18]. A two-step protocol was therefore implemented, beginning with the treatment of **6** with BCl_3·SMe_2 in CH_2Cl_2 for 30 min at ambient temperature [19]. This successfully generated the chloroacetal **7** exclusively as the α-anomer in 46% isolated yield, which was then exposed to a mixture of DMF and saturated aqueous $NaHCO_3$ to give the desired lactol **8** in 92% yield. Finally, preparation of the trichloroacetimidate donor was straightforward and proceeded in almost quantitative yield (99%, exclusively the α-anomer), thereby completing the synthesis sequence in 24% over 6 steps. For a comparative selectivity analysis, the C6-OBn substituted derivative **13** was also required: this was accessed from commercial 2,3,4,6-tetra-*O*-benzyl-D-glucopyranose, as previously described [10a], in an α:β ratio of 11:1 as determined by ^{1}H NMR spectroscopy (see Table 1) (Scheme 1).

To glean insights into the conformational behavior of the 6-fluoro oxocarbenium ion that is central to this study (Fig. 1, Scheme 2) the corresponding gluconolactone was selected as a mimic for NMR conformer population analysis. Lactones of this nature have frequently been employed as convenient models for the study of ephemeral oxocarbenium ions on account of the planar geometry around the O–C–O fragment and the partial positive charge on the pyranose-oxygen (Scheme 2, left) [20]. It was envisaged that analyses of these systems might also provide useful information regarding the conformational equilibrium that results from rotation around the C5–C6 bond: the populations of the three limiting staggered conformations partitioned by 120° were of particular interest (Scheme 2, right. **I**, **II** and **II**, Fig. 1). Based on the findings that 2,3,4,6-tetra-*O*-benzyl-D-gluconolactone (**11**) exists in a $^4H_3$ conformation, rather than a $B_{2,5}$ boat [21], the half-chair transition states were preferentially considered.

To perform the solution phase conformer population analysis, the experimental $^3J_{HH}$ coupling constants were required. Compound **10** was synthesized starting from structure **8** in 92% by Albright–Goldman oxidation, and the $^3J_{HH}$ constants were determined to be 2.9 and 1.7 Hz. For compound **11** the literature values of 3.2 Hz and 2.4 Hz were used [22]. Finally, a simplified structural model was employed (**12**) (Scheme 2) and the theoretical $^3J^g_{HH}$ and $^3J^a_{HH}$ were calculated based on estimated group electronegativities of F = 1.71, OBn = 1.20, OAc = 1.57 and CH_2OMe = 0.13 [23]. Under these assumptions, molar fractions (χ_I, χ_{II}, χ_{III}) of (0.74, 0.23, 0.03)

Table 1
Summary of selectivity data for donors **9** and **13** at different temperatures.

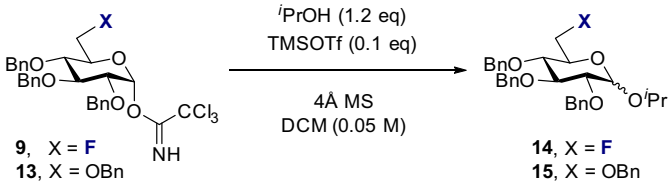

Donor	T (K)[a]	$r_{\beta\alpha}$	$\sigma_{\beta\alpha}$[b]	$r'_{\beta\alpha}$	$r_{\beta\alpha}/r'_{\beta\alpha}$
9 (X=F)	299.15 (25)	1.14	0.07 (6.5%)	0.83	0.73
9	274.15 (0)	1.08[c]	0.09 (8.6%)	1.07	0.99
9	244.15 (−30)	1.52[c]	0.08 (5.5%)	1.56	1.03
9	214.15 (−60)	2.58	0.13 (5.2%)	2.53	0.98
9	194.15 (−80)	3.79	0.10 (2.7%)	3.80	1.00
13 (X=OBn)	299.15 (25)	1.22	0.06 (4.7%)	1.24	1.01
13	274.15 (0)	1.44	0.10 (6.7%)	1.69	1.18
13	244.15 (−30)	3.27	0.19 (5.7%)	2.68	0.82
13	214.15 (−60)	5.52	0.22 (4.1%)	4.84	0.88
13	194.15 (−80)	6.82	0.33 (4.9%)	7.94	1.16

[a] In parentheses, values in °C.
[b] Relative standard deviations $\sigma_{\beta\alpha}/r_{\beta\alpha}$.
[c] Two reactions run at 0.05 M and two reactions run at 0.03 M.

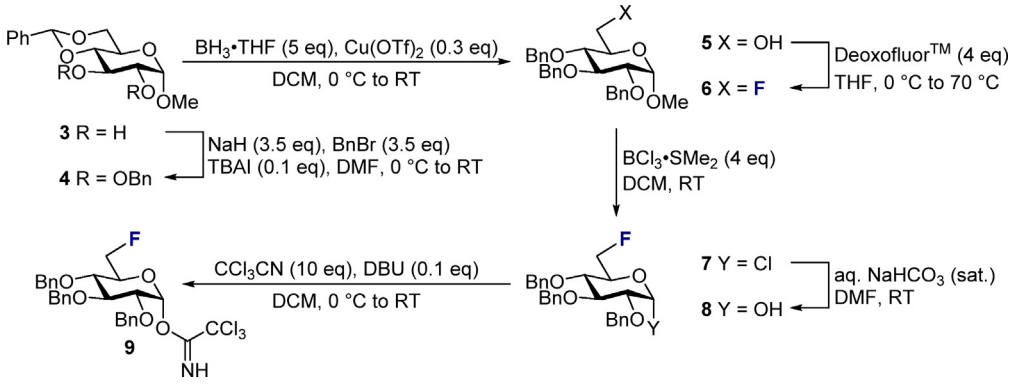

Scheme 1. Synthetic route to fluorinated glycosyl donor **9**.

and (0.79, 0.20, 0.01) were determined for lactones **10** and **11**, respectively. For compound **10**, χ_{II} may also be estimated based on the $^3J_{CF}$ coupling constant according to $\chi_{II} = (^3J^{exp}_{CF} - {}^3J^{g}_{CF})/(^3J^{a}_{CF} - {}^3J^{g}_{CF})$ with standardized values of $^3J^{g}_{CF} = 1.2 \pm 1.0$ Hz and $^3J^{a}_{CF} = 11.2 \pm 2.0$ Hz [24]. Thus, for $^3J^{exp}_{CF} = 5.8$ Hz a higher population $\chi_{II} = 0.46$ results. These data indicate that the major solution phase conformer has the highly electronegative fluorine substituent in close proximity to the electron deficient pyranose oxygen (**I**): this is consistent with an earlier conformational analysis of 6-deoxy-6-fluoro-D-glucose [25]. It is interesting to note that an elegant reactivity study by Bols and co-workers implicated rotamer **I** as being the most reactive in a study of glycoside hydrolysis [26]. This study indicates that both donors (X=F or OBn) display comparable conformational behavior with respect to rotation about C5–C6. This is consistent with the working stereoelectronic hypothesis and can be rationalized based on hyperconjugative interactions ($\sigma_{C-H} \rightarrow \sigma^*_{C-X}$; X=F or OBn)—albeit a stronger bias was initially expected for the fluorinated system. For conformers **I** and **II**, a stabilizing Coulombic interaction can also be invoked on account of the proximity of the partially negatively charged substituent X (X=F or OBn) to the pyranose oxygen: this should be more pronounced in the $^3H_4$ half-chair than in the $^4H_3$ half-chair (closer spatial alignment; Scheme 3).

Having analyzed the solution phase conformational behavior of the oxocarbenium ion mimics **10** and **11** by NMR spectroscopy, attention was then turned to the performance of the glycosyl donor in a model glycosylation reaction. To that end, the trichloroacetimidate donors **9** and **13** were independently subjected to standard, commonly employed glycosylation conditions using iPrOH as a glycosyl acceptor and TMSOTf as Lewis acid catalyst. Furthermore, in order to preclude solvent participation, all

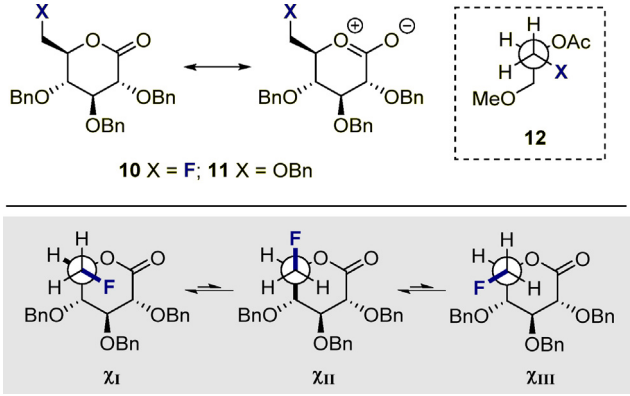

Scheme 2. Lactones **10** and **11** used as models for ^{1}H NMR conformer population analysis.

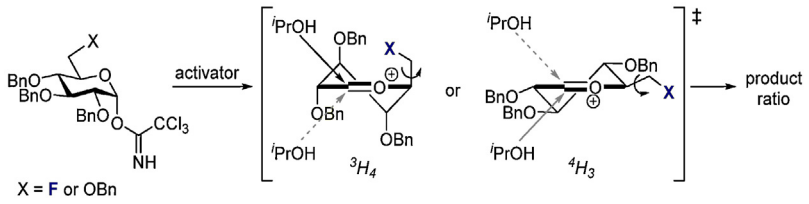

Scheme 3. Tentative S_N1 type glycosylation mechanism with β-TS ($^3H_4$) and α-TS ($^4H_3$) and possible nucleophile trajectories (solid and dashed lines). The solid gray arrows corresponds to trajectories that are consistent with the Fürst–Plattner rule (solid gray).

experiments were conducted in CH_2Cl_2 (c 0.05 M). After quenching the reaction mixtures by addition of NEt_3 and subsequent concentration under reduced pressure, the selectivities [β:α ratios ($r_{\beta\alpha}$)] were determined directly either by ^{19}F or ^1H NMR spectroscopy for **14** and **15**, respectively (Table 1). Each experiment was repeated at least 3 times to ensure reproducibility and estimate the accuracy of the method in the form of standard deviations ($\sigma_{\beta\alpha}$); these ranged from 2.7 to 8.6%. Moreover, the glycosylation reactions were run at five discrete temperatures, ranging from ambient temperature to −80 °C in order to derive the thermodynamic parameters $\Delta\Delta H_{\beta\alpha}$ and $\Delta\Delta S_{\beta\alpha}$. These data are summarized in Table 1 and include the predicted selectivity ratios ($r'_{\beta\alpha}$) as determined based on the aforementioned values of $\Delta\Delta H_{\beta\alpha}$ and $\Delta\Delta S_{\beta\alpha}$.

Whereas both donors performed comparably at ambient temperature with $r_{\beta\alpha}$ values of 1.14 ± 0.07 and 1.22 ± 0.06 for **14** and **15**, respectively, a clear selectivity differences were noted at lower temperatures (6-OBn > 6-F). To extrapolate the thermodynamic parameters $\Delta\Delta H_{\beta\alpha}$ and $\Delta\Delta S_{\beta\alpha}$, the data was then subjected to further investigations on the basis of an Eyring plot according to the following equation [27].

$$\ln(r_{\beta\alpha}) = -\Delta\Delta H_{\beta\alpha}^{\ddagger}(\mathrm{RT})^{-1} + \Delta\Delta S_{\beta\alpha}^{\ddagger} \times R^{-1} \quad (1)$$

By means of linear regression ($\ln(r_{\beta\alpha}) \sim T^{-1}$), the enthalpic ($\Delta\Delta H_{\beta\alpha}^{\ddagger}$) and entropic ($\Delta\Delta S_{\beta\alpha}^{\ddagger}$) contributions to the difference in free energy between the β- and α-transition states ($\Delta\Delta G_{\beta\alpha}^{\ddagger} = \Delta G_{\beta}^{\ddagger} - \Delta G_{\alpha}^{\ddagger}$) were calculated to be -7.02 ± 0.17 kJ mol^{-1} and -25.0 ± 0.8 J mol^{-1} K^{-1} for **14**, and -8.55 ± 1.06 kJ mol^{-1} and -26.8 ± 4.5 J mol^{-1} K^{-1} for **15** with correlation coefficients R^2 of 0.99 and 0.96, respectively (Fig. 2). As the selectivity ratio ($r_{\beta\alpha}$) for product **14** was higher at 25 °C than at 0 °C, this data point was not considered in the initial analysis. This reversal in selectivity could point toward a general change in mechanism, but in the absence of additional data points this is purely speculative. It is important to note that when the data point was included, slightly different $\Delta\Delta H_{\beta\alpha}^{\ddagger}$ and $\Delta\Delta S_{\beta\alpha}^{\ddagger}$ values of -6.00 ± 0.72 kJ mol^{-1} and -20.0 ± 3.1 J mol^{-1} K^{-1} were obtained with a goodness of fit of 0.95. Next, predicted selectivity ratios $r'_{\beta\alpha}$ were calculated based on all values derived using rearranged Eq. (1) [28]. These selectivity ratios closely matched the experimental values, as evidenced by the ratio ($r_{\beta\alpha}/r'_{\beta\alpha}$) ranging from 0.88 to 1.16.

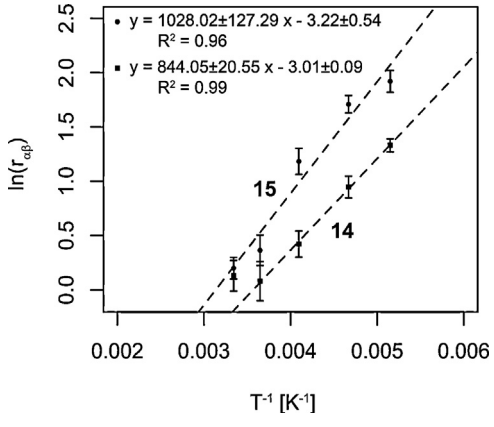

Fig. 2. Eyring plot of the selectivity data summarized in Table 1. Error bars are presented as $2 \times \sigma'_{\beta\alpha}$ with $\sigma'_{\beta\alpha} = \sigma_{\beta\alpha}/r_{\beta\alpha}$.

For analysis of the entropic parameter $\Delta\Delta S_{\beta\alpha}^{\ddagger}$ a fully dissociative, S_N1-type mechanism was assumed (Scheme 3), proceeding via an intermittent oxocarbenium ion followed by reaction with the acceptor. This is consistent with the observed erosion of the β:α ratio associated with reaction of the (α-enriched) trichloroacetimidate donor to form the isopropyl-glycoside (i.e. consistent with a mechanism which has significant S_N1 character) [see Ref. [10c]]. In contrast, a reaction with significant S_N2-character would be expected to furnish a product β:α ratio that reflects the associated inversion of configuration at the anomeric centre (i.e. an inverted β:α ratio of that of the donors employed). In the case of donor (α)-**9**, almost exclusive β-selectivity would be expected.

In this S_N1 paradigm, a negative entropy of activation for the associative second step can reasonably be assumed ($\Delta S^{\ddagger} < 0$). The finding that ($\Delta\Delta S_{\beta\alpha}^{\ddagger} = \Delta S_{\beta}^{\ddagger} - \Delta S_{\alpha}^{\ddagger}) < 0$ implicates $\Delta S_{\beta}^{\ddagger} < \Delta S_{\alpha}^{\ddagger} < 0$, i.e. that for both substitutions (X=F or OBn) the β-TS ($^3H_4$) is more constrained than the corresponding α-TS ($^4H_3$).

Moreover, since the donors vary only at the C6 locus, differences in $\Delta\Delta S_{\beta\alpha}^{\ddagger}$ are expected to primarily stem from rotational flexibility about the C5–C6 bond. The finding that $\Delta\Delta S_{\beta\alpha}^{\ddagger}$(**14**) = −25.0±0.8 J mol^{-1} K^{-1} is almost equal to the value of $\Delta\Delta S_{\beta\alpha}^{\ddagger}$(**15**) = −26.8±4.5 J mol^{-1} K^{-1} is also in line with comparable solution phase populations of the model systems **10** and **11**. It is therefore postulated that the difference in selectivity observed between the C6-F (**9**) and C6-OBn (**13**) glycosyl donors result from enthalpic contributions.

3. Conclusion

The selectivity of two structurally similar glucose-derived donors differing only at the 6-position (X=F versus OBn) was studied in a model glycosylation reaction with ^{i}PrOH at varying temperatures. At −80 °C the highest selectivities were observed with β:α ratios of 3.79:1 and 6.82:1 for donors **9** (X=F) and **13** (X=OBn), respectively. This selectivity data was then subjected to an Eyring analysis to extrapolate the enthalpic ($\Delta\Delta H_{\beta\alpha}^{\ddagger}$) and entropic ($\Delta\Delta S_{\beta\alpha}^{\ddagger}$) parameters associated with the transition states that lead to the β- or α-anomer. Whereas the relative entropic destabilization of the β-TS versus the α-TS was comparable for both donors, the enthalpic stabilization of the β-TS versus the α-TS was larger for the 6-benzyloxy system. This comparable values for $\Delta\Delta S_{\beta\alpha}^{\ddagger}$ support the findings that rotation around the C5–C6 bond is equally hindered in both oxocarbernium ion mimics **10** and **11**. This can be rationalized by invoking stabilizing hyperconjugative interactions ($\sigma_{C-H} \rightarrow \sigma^*_{C-X}$; X=F or OBn). Consequently,

selectivity differences likely arise from variances in enthalpic contributions ($\Delta\Delta H_{\beta\alpha}^{\ddagger}$) and may be tentatively rationalized by electronic shielding of the planar oxocarbenium moiety. A possible rationale for this may be attributed to the lower polarizability of fluorine (versus OBn) such that nucleophilic attack in the β-TS is enthalpically more costly for X=F than X=OBn. Intriguingly, molecular editing at the 6-position of glucose [OBn → F] is accompanied by a reduction in β-selectivity on account of the electronic shielding effect of this small substituent. Whilst rotamer **I** is equally populated for X=F or OBn in a model system, and the intermediate oxocarbenium ion likely resembles the $^3H_4$ in both scenarios, the study has demonstrated that fluorine disfavors top face (β)-attack more strongly than OBn. Efforts to further explore the utility of fluorine as a steering group in chemical glycosylation are currently ongoing.

4. Experimental

4.1. 2,3,4-Tri-O-benzyl-6-deoxy-6-fluoro-α-D-glucopyranosyl trichloroacetimidate 9

At 0 °C and under Ar, 0.1 mL (0.06 mmol, 0.1 eq.) of a 0.6 M stock solution of DBU in CH_2Cl_2 was added to a solution of 2,3,4-tri-*O*-benzyl-α/β-D-glucopyranoside (**8**) (30 mg, 0.6 mmol, 1.0 eq.) and trichloroacetonitrile (0.7 mL, 6 mmol, 10.0 eq..) in CH_2Cl_2 (1.2 mL). After 5 min the solution was allowed to warm to room temperature and stirred for 2 h. The solvent was evaporated under reduced pressure. Fast filtration over silica gel (SiO_2, Cyhx/EtOAc 10:1) afforded trichloroacetimidate (**9**) as colorless oil (354 mg, 99%), mainly as the α-anomer. **R_f** (Cyhx/EtOAc 4:1) = 0.69; **m/z** (ESI) found: 618.0984 $(M+Na)^+$, $C_{29}H_{29}NO_5Cl_3FNa$ requires 618.0988; $[\alpha]_D^{26}$ = +48 (*c* 1.00 in CH_2Cl_2); **ν_{max}** (neat)/cm^{-1} 3338w, 3031w, 2871w, 1736w, 1670m, 1497w, 1454m, 1360m, 1287m, 1210w, 1156m, 1072s, 1005s, 908m, 859m, 830m, 795s, 737s, 698s; **^{1}H NMR** (400 MHz, $CDCl_3$) δ = 8.61 (1*H*, s, NH), 7.40–7.26 (15*H*, m, ar. H), 6.42 (1*H*, d, *J* = 4 Hz, H-C1), 4.98 (1*H*, d, *J* = 11 Hz, $BnCH_2$), 4.93 (1*H*, d, *J* = 11 Hz, $BnCH_2$), 4.85 (1*H*, d, *J* = 11 Hz, $BnCH_2$), 4.75 (1*H*, d, *J* = 12 Hz, $BnCH_2$), 4.69 (1*H*, d, *J* = 13 Hz, $BnCH_2$), 4.64 (1*H*, d, *J* = 11 Hz, $BnCH_2$), 4.64 (1*H*, ddd, *J* = 48, 11, 3 Hz, H-C6), 4.56 (1*H*, ddd, *J* = 48, 10, 2 Hz, H-C6), 4.08 (1*H*, t, *J* = 9 Hz, H-C3), 4.03–3.87 (1*H*, m, H-C5), 3.75 (1*H*, dd, *J* = 9, 3 Hz, H-C4), 3.74–3.65 (1*H*, m, H-C2) ppm; **^{13}C NMR** (101 MHz, $CDCl_3$) δ = 161.2 (C7), 138.4 (iPh), 137.8 (iPh), 137.7 (iPh), 128.5 (Ph), 128.4 (Ph), 128.4 (Ph), 128.1 (Ph), 128.0 (Ph), 128.0 (Ph), 127.8 (Ph), 127.7 (Ph), 127.7 (Ph), 94.1 (C1), 91.1 (C8), 81.4 (d, $^1J_{CF}$ = 174 Hz, C6), 81.1 (C3) 79.2 (C2), 75.9 (d, $^3J_{CF}$ = 6 Hz, C4), 75.7 ($BnCH_2$), 75.5 ($BnCH_2$), 73.0 ($BnCH_2$), 72.6 (d, $^2J_{CF}$ = 18 Hz, C5) ppm; **^{19}F NMR** (282 MHz, $CDCl_3$) δ = −234.93 (td, $^2J_{FH}$ = 48 Hz, $^3J_{FH}$ = 30 Hz) ppm.

4.2. 1-O-Isopropyl-2,3,4-tri-O-benzyl-6-deoxy-6-fluoro-α/β-D-glucopyranoside 14

In a 10 mL Schlenk-tube containing 4Å molecular sieves 2,3,4-tri-*O*-benzyl-6-deoxy-6-fluoro-D-glucopyranosyl trichloroacetimidate (**9**) (25 mg, 0.04 mmol, 1.0 eq.) was dissolved in CH_2Cl_2 (0.7 mL) under Ar. After cooling to −90 °C, 0.1 mL (0.05 mmol, 1.2 eq.) of an ^{i}PrOH stock solution (0.5 M in CH_2Cl_2) was added followed by 0.1 mL (0.005 mmol, 0.1 eq.) of a TMSOTf stock solution (0.05 M in CH_2Cl_2). Upon reaction completion NEt_3 was added for quenching and the solvent was removed under reduced pressure. The product was purified by column chromatography (SiO_2, Cyhx/EtOAc 10:1) affording 1-*O*-isopropyl-2,3,4-tri-*O*-benzyl-6-deoxy-6-fluoro-α/β-D-glucopyranoside (**14**) as a white solid (15 mg, 76%, α:β = 1:10.7).

R_f (Cyhx/EtOAc 4:1) = 0.58; **m.p.** 66 °C; **m/z** (ESI) found: 517.2353 $(M+Na)^+$, $C_{30}H_{35}FO_5Na$ requires 517.2361; **ν_{max}** (neat)/cm^{-1} 3030w, 2972w, 2867w, 1497w, 1454m, 1382w, 1357w, 1209w, 1069br, 1029br, 1013br, 912w, 736s, 698s; **^{1}H NMR** (400 MHz, $CDCl_3$) δ = 7.35–7.19 (15*H*, m, ar. H), 4.93 (1*H*, d, *J* = 11 Hz, $BnCH_2$), 4.90 (1*H*, d, *J* = 11 Hz, $BnCH_2$), 4.83 (1*H*, d, *J* = 11 Hz, $BnCH_2$), 4.75 (1*H*, d, *J* = 11 Hz, $BnCH_2$), 4.66 (1*H*, d, *J* = 11 Hz, $BnCH_2$), 4.64–4.39 (2*H*, m, H-C6 β), 4.55 (1*H*, d, *J* = 11 Hz, $BnCH_2$), 4.44 (1*H*, d, *J* = 8 Hz, H-C1β), 3.98 (1*H*, sept, *J* = 6 Hz, H-C7β), 3.83 (1*H*, sept, *J* = 6 Hz, H-C7α), 3.79 (1*H*, dddd, *J* = 30, 10, 3, 2 Hz, H-C5α), 3.62 (1*H*, t, *J* = 9 Hz, H-C3β), 3.50 (1*H*, t, *J* = 9 Hz, H-C4β), 3.41 (1*H*, dddd, *J* = 25, 10, 4, 2 Hz, H-C5β), 3.39 (1*H*, dd, *J* = 9, 8 Hz, H-C2β), 1.26 (3*H*, d, *J* = 6 Hz, H-C8β), 1.20 (3*H*, d, *J* = 6 Hz, H-C8β), 1.18 (3*H*, d, *J* = 6 Hz, H-C8α), 1.14 (3*H*, d, *J* = 6 Hz, H-C8α) ppm, only some characteristic α-signals are reported; **^{13}C NMR** (101 MHz, $CDCl_3$) δ = 138.9 (iPhα), 138.6 (iPhβ), 138.5 (iPhβ), 138.2 (iPhα), 138.1 (iPhα), 138.0 (iPhβ), 128.6 (Ph), 128.6 (Ph), 128.6 (Ph), 128.5 (Ph), 128.5 (Ph), 128.3 (Ph), 128.3 (Ph), 128.2 (Ph), 128.1 (Ph), 128.0 (Ph), 128.0 (Ph), 127.8 (Ph), 127.8 (Ph), 127.7 (Ph), 102.2 (C1β), 95.0 (C1α), 84.6 (C3β), 82.3 (C2β), 82.2 (d, $^1J_{CF}$ = 174 Hz, C6β), 80.1 (d, $^1J_{CF}$ = 205 Hz, C6α), 76.8 (d, $^3J_{CF}$ = 6 Hz, C4β), 77.0 (d, $^3J_{CF}$ = 6 Hz, C4α), 75.8 ($BnCH_2$ α and β), 75.4 ($BnCH_2$α), 75.1 ($BnCH_2$β), 74.9 ($BnCH_2$β), 73.0 (d, $^2J_{CF}$ = 18 Hz, C5β), 73.3 ($BnCH_2$α), 72.6 (C7β), 69.9 (d, $^2J_{CF}$ = 18 Hz, C5α), 69.4 (C7α), 23.8 (C8β), 23.3 (C8α), 22.3 (C8β), 21.3 (C8α) ppm; **^{19}F NMR** (282 MHz, $CDCl_3$) δ = −232.34 (td, $^2J_{FH}$ = 48 Hz, $^3J_{FH}$ = 25 Hz β-anomer), −234.26 (td, $^2J_{FH}$ = 48 Hz, $^3J_{FH}$ = 30 Hz, α-anomer) ppm.

Acknowledgements

We acknowledge generous financial support from the Swiss National Science Foundation (P2EZP2-148757), the DFG (SFB 858 and Excellence Cluster EXC 1003 "Cells in Motion—Cluster of Excellence") and the European Research Council (ERC-2013-StG Starter Grant. Project number 336376-ChMiFluorS).

Appendix A. Supplementary data

Supplementary data associated with this article can be found, in the online version, at http://dx.doi.org/10.1016/j.jfluchem.2015.06.004.

References

[1] (a) For selected reviews on organofluorine chemistry see D. O'Hagan, Chem. Soc. Rev. 37 (2008) 308–319;
(b) S. Purser, P.R. Moore, S. Swallow, V. Gouverneur, Chem. Soc. Rev. 37 (2008) 320–330;
(c) V. Gouverneur, K. Müller (Eds.), Fluorine in Pharmaceutical and Medicinal Chemistry, Imperial College Press, London, 2010;
(d) L.E. Zimmer, C. Sparr, R. Gilmour, Angew. Chem. Int. Ed. 50 (2011) 11860–11871.
[2] (a) For selected reviews on glycochemistry see, Nature Insight: Glycochemistry and Glycobiology, 446 (2007) 999–1051.
(b) N.S. Sampson, M. Mrksich, C.R. Bertozzi, Proc. Natl. Acad. Sci. U.S.A. 98 (2001) 12870–12871;
(c) C.R. Bertozzi, L.L. Kiessling, Science 291 (2001) 2357–2364;
(d) T.J. Boltje, T. Buskas, G.-J. Boons, Nat. Chem. 1 (2009) 611–622;
(e) P.H. Seeberger, Nat. Chem. Biol. 5 (2009) 368–372.
[3] For an excellent review of carbohydrate inspired glycomimetic drug development see B. Ernst, J.L. Magnani, Nat. Rev. Drug Discovery, 8 (2009) 661–677.
[4] G.T. Giuffredi, V. Gouverneur, B. Bernet, Angew. Chem. Int. Ed. 52 (2013) 10524–10528.
[5] (a) For selected examples of fluorinated carbohydrates see I.P. Street, C.R. Armstrong, S.G. Withers, Biochemistry, 25 (1986) 6021–6027;
(b) S.G. Withers, D.J. MacLennan, I.P. Street, Carbohydr. Res. 154 (1986) 127–144;
(c) M.D. Burkart, Z. Zhang, S.-C. Hung, C.-H. Wong, J. Am. Chem. Soc. 119 (1997) 11743–11746;

(d) M. Albert, B.J. Paul, K. Dax, Synlett 9 (1999) 1483–1485;
(e) T. Miyazaki, T. Sakakibara, H. Sato, Y. Kajihara, J. Am. Chem. Soc. 121 (1999) 1411–1412;
(f) A.G. Watts, I. Damager, M.L. Amaya, A. Buschiazzo, P. Alzari, A.C. Frasch, S.G. Withers, J. Am. Chem. Soc. 125 (2003) 7532–7533;
(g) C.A. Tarling, S.G. Withers, Carbohydr. Res. 339 (2004) 2487–2497;
(h) V. Subramaniam, S.S. Gurcha, G.S. Besra, T.L. Lowary, Bioorg. Med. Chem. 13 (2005) 1083–1094;
(i) D. Crich, L. Li, J. Org. Chem. 72 (2007) 1681–1690;
(j) H.A. Chokhawala, H. Cao, H. Yu, X. Chen, J. Am. Chem. Soc. 129 (2007) 10630–10631;
(k) D. Benito, M.I. Matheu, A. Morère, Y. Díaz, S. Castillón, Tetrahedron 64 (2008) 10906–10911;
(l) B.R. Rempel, S.G. Withers, Aust. J. Chem. 62 (2009) 590–599;
(m) S.A. Allman, H.H. Jensen, B. Vijayakrishnan, J.A. Garnett, E. Leon, Y. Liu, D.C. Anthony, N.R. Sibson, T. Feizi, S. Matthews, B.G. Davis, ChemBioChem 10 (2009) 2522–2529;
(n) G.T. Giuffredi, S. Purser, M. Sawicki, A.L. Thompson, V. Gouverneur, Tetrahedron: Asymmetry 20 (2009) 910–920;
(o) O. Boutureira, F. D'Hooge, M. Fernandez-Gonzalez, G.J.L. Bernardes, M. Sanchez-Navarro, J.R. Koeppe, B.G. Davis, Chem. Commun. 46 (2010) 8142–8144;
(p) A. Hoffmann-Röder, A. Kaiser, S. Wagner, N. Gaidzik, D. Kowalczyk, U. Westerlind, B. Gerlitzki, E. Schmitt, H. Kunz, Angew. Chem. Int. Ed. 49 (2010) 8498–8503;
(q) S. Wagner, C. Mersch, A. Hoffmann-Röder, Chem. Eur. J. 16 (2010) 7319–7330;
(r) S. Bresciani, T. Lebl, A.M.Z. Slawin, D. O'Hagan, Chem. Commun. 46 (2010) 5434–5436;
(s) A. Ioannou, E. Cini, R.S. Timofte, S.L. Flitsch, N.J. Turner, B. Linclau, Chem. Commun. 47 (2011) 11228–11230;
(t) M.J. Corr, D. O'Hagan, J. Fluorine Chem. 155 (2013) 72–77;
(u) L. Mtashobya, L. Quiquempoix, B. Linclau, J. Fluorine Chem. 171 (2014) 92–96;
(v) K.A. van Straaten, J.R. Kuttiyatveetil, C.M. Sevrain, S.A. Villaume, J. Jimenez-Barbero, B. Linclau, S.P. Vincent, D.A.R. Sanders, J. Am. Chem. Soc. 137 (2015) 1230–1244;
(w) Also see the special edition Fluoro Sugars, Carbohydr. Res. 327 (2000) 1.
[6] (a) M.N. Namchuck, J.D. McCarter, A. Becalski, T. Andrews, S.G. Withers, J. Am. Chem. Soc. 122 (2000) 1270–1277;
(b) M.D. Percival, S.G. Withers, Biochemistry 31 (1992) 505–512.
[7] (a) T. Oberbillig, C. Mersch, S. Wagner, A. Hoffmann-Röder, Chem. Commun. 48 (2012) 1487–1489;
(b) T. Oberbillig, H. Löwe, A. Hoffmann-Röder, J. Flow Chem. 2 (2012) 83–86.
[8] (a) B.R. Landau, C.L. Spring-Robinson, R.F. Muzic, N. Rachdaoui, D. Rubin, M.S. Berridge, W.C. Schumann, V. Chandramouli, T.S. Kern, R. Ismail-Beigi, Am. J. Physiol. Endocrinol. Metab. 293 (2007) 237–245;
(b) T.R. Neal, W.C. Schumann, M.S. Berridge, B.R. Landau, J. Labelled Compd. Radiopharm. 48 (2005) 845–854.
[9] (a) For theoretical treatments of the gauche effect see L. Goodman, H. Gu, V. Pophristic, J. Phys. Chem. A, 109 (2005) 1223–1229;
(b) P.R. Rablen, R.W. Hoffmann, D.A. Hrovat, W.T. Borden, J. Chem. Soc., Perkin Trans. 2 8 (1999) 1719–1726;
(c) D.Y. Buissonnneaud, T. van Mourik, D. O'Hagan, Tetrahedron 66 (2010) 2196–2202;
(d) M. Baranac-Stojanović, RSC Adv. 4 (2014) 43834–43838;
(e) For a recent study of the gauche effect in 2,3-difluorobutane see S.J. Fox, S. Gourdain, A. Coulthurst, C. Fox, I. Kuprov, J.W. Essex, C.K. Skylaris, B. Linclau, Chem. Eur. J. 21 (2015) 1682–1691.
[10] (a) C. Bucher, R. Gilmour, Angew. Chem. Int. Ed. 49 (2010) 8724–8728;
(b) C. Bucher, R. Gilmour, Synlett (2011) 1043–1046;
(c) E. Durantie, C. Bucher, R. Gilmour, Chem. Eur. J. 18 (2012) 8208–8215.
[11] D. Crich, Acc. Chem. Res. 43 (2010) 1144–1153.
[12] (a) R.J. Woods, C.W. Andrews, J.P. Bowen, J. Am. Chem. Soc. 114 (1992) 859–864;
(b) J.A.C. Romero, S.A. Tabacco, K.A. Woerpel, J. Am. Chem. Soc. 122 (2000) 168–169.
[13] M. Matwiejuk, J. Thiem, Chem. Commun. 47 (2011) 8379–8381.
[14] R. Johnson, D. Olsson, U. Ellervik, J. Org. Chem. 73 (2008) 5226–5232.
[15] P. Ková, H.J.C. Yeh, G.L. Jung, J. Carbohydr. Chem. 6 (1987) 423–439.
[16] P.A. Messina, K.C. Mange, W.J. Middleton, J. Fluorine Chem. 42 (1989) 137–143.
[17] A.M. Esmurziev, N. Simic, B.H. Hoff, E. Sundby, J. Carbohydr. Chem. 29 (2010) 348–367.
[18] (a) For select attempted protocols consider M. Matwiejuk, J. Thiem, Eur. J. Org. Chem. (2011) 5860–5878;
(b) M.E. Jung, M.A. Lyster, J. Org. Chem. 42 (1977) 3761–3764;
(c) A. Kumar, V.R. Doddi, Y.D. Vankar, J. Org. Chem. 73 (2008) 5993–5995.
[19] S. Halazy, V. Berges, A. Ehrhard, C. Danzin, J. Fluorine Chem. 59 (1992) 185–192.
[20] S. Chamberland, J.W. Ziller, K.A. Woerpel, J. Am. Chem. Soc. 127 (2005) 5322–5323.
[21] J. Gratien, M.-P. Heck, C. Mioskowski, Carbohydr. Res. 343 (2008) 18–30.
[22] S.Y. Kang, K.-S. Song, J. Lee, S.-H. Lee, J. Lee, Bioorg. Med. Chem. 18 (2010) 6069–6079.
[23] S. Hamman, C. Béguin, C. Charlon, C. Luu-Duc, Org. Magn. Reson. 21 (1983) 361–366.
[24] A. Dahbi, S. Hamman, C.G. Béguin, Magn. Reson. Chem. 24 (1986) 337–342.
[25] R.J. Abraham, E.J. Chambers, W.A. Thomas, Magn. Reson. Chem. 30 (1992) S60–S65.
[26] H.H. Jensen, L.U. Nordstrøm, M. Bols, J. Am. Chem. Soc. 126 (2004) 9205–9213.
[27] H. Buschmann, H.-D. Scharf, N. Hoffmann, P. Esser, Angew. Chem. Int. Ed. 30 (1991) 477–515.
[28] $r'_{\beta\alpha} = \exp(-\Delta\Delta H_{\beta\alpha}^{\ddagger} \times (RT)^{-1} + \Delta\Delta S_{\beta\alpha}^{\ddagger} \times R^{-1})$.